

# Structure of xylogalacturonan fragments from watermelon cell-wall pectin. Endopolygalacturonase can accommodate a xylosyl residue on the galacturonic acid just following the hydrolysis site

Andrew Mort,<sup>a,\*</sup> Yun Zheng,<sup>a</sup> Feng Qiu,<sup>b</sup> Manfred Nimtz<sup>c</sup> and Gianna Bell-Eunice<sup>a</sup>

<sup>a</sup>Department of Biochemistry and Molecular Biology, Oklahoma State University, Stillwater, OK, USA

<sup>b</sup>Department of Chemistry, CUNY Graduate Center and College of Staten Island, Staten Island, NY, USA

<sup>c</sup>GBF, Gesellschaft für Biotechnologische Forschung mbH, Mascheroder Weg 1, D-38124 Braunschweig, Germany

Received 12 November 2007; received in revised form 7 March 2008; accepted 12 March 2008

Available online 20 March 2008

**Abstract**—A combination of xylogalacturonan (XGA), homogalacturonan, and rhamnogalacturonan was extracted from watermelon fruit cell walls with 0.1 M NaOH. In contrast to the resistance of xylogalacturonans from most other sources to endopolygalacturonase (EPG), about 50% of the extracted XGA could be converted into oligosaccharides by EPG digestion with a commercial EPG from Megazyme International. The oligosaccharides were fractionated by ion-exchange chromatography, and their structures were investigated by mass spectrometry and NMR spectroscopy. The smallest oligosaccharide was  $\beta$ -D-Xylp-(1→3)- $\alpha$ -D-GalAp-(1→4)- $\alpha$ -D-GalAp-(1→4)- $\alpha$ -D-GalAp-(1→4)-GalAp. The most abundant was  $\beta$ -D-Xylp-(1→3)- $\alpha$ -D-GalAp-(1→4)- $\alpha$ -D-GalAp-(1→4)-( $\beta$ -D-Xylp-(1→3)- $\alpha$ -D-GalAp-(1→4))- $\alpha$ -D-GalAp-(1→4)- $\alpha$ -D-GalAp-(1→4)-GalAp. Given that the non-reducing ends of the oligosaccharides often were xylosylated GalA residues, and that fungal EPG digests homogalacturonans between the third and fourth GalA bound to the enzyme, it appears that EPG can accommodate a xylosylated GalA in the site that binds the fourth GalA. Since all of the oligosaccharides characterized had three unsubstituted GalA residues at their reducing ends, the enzyme appears not to accommodate xylosylated residues in the first three sugar-binding sites. Thus, XGA regions with fewer than three unsubstituted residues between branch points will be resistant to EPG. The EPG-susceptible XGA was not recovered from cell walls prepared using phosphate buffer for the homogenization of the watermelon tissue, probably because it was degraded by endogenous watermelon EPG and lost during isolation of the walls. Use of Tris-buffered phenol during wall isolation to prevent enzyme action caused some amidation of GalA residues with Tris.

© 2008 Elsevier Ltd. All rights reserved.

**Keywords:** Xylogalacturonan; Watermelon; Endopolygalacturonase; Structure; Specificity; NMR spectroscopy

## 1. Introduction

The region of pectin designated xylogalacturonan (XGA) has been gaining more attention recently. XGA was first reported in an alkali extract of pine pollen<sup>1</sup> and found to have a homogalacturonan backbone with frequent single xylose residues linked  $\beta$ -(1→3) to about half of the galacturonic acid residues. Gum trag-

acanth has a similar structure but with galactose or fucose linked to O-2 of some of the xylose residues.<sup>2</sup> Schols et al.<sup>3</sup> found that part of the so-called ‘modified hairy region’ of apple pectin is XGA. They also found evidence of XGAs being present in several other fruits and vegetables.<sup>4</sup> Yu and Mort reported its presence in watermelon fruit.<sup>5</sup> Albersheim et al. proposed that XGAs are only present in fruits,<sup>6</sup> since XGA had not been found in walls from sycamore suspension cultures and it had only been reported in fruits to that point. However, Kikuchi et al.<sup>7</sup> reported the presence of

\* Corresponding author. Tel.: +1 405 744 6197; fax: +1 405 744 7799; e-mail: [andrew.mort@okstate.edu](mailto:andrew.mort@okstate.edu)

XGA in cultured carrot cells, Zandleven et al.<sup>8</sup> reported the presence of XGAs in multiple organs of Arabidopsis, and we find it in cotton suspension culture cell walls.<sup>9</sup> In some XGAs, such as that from pea hulls, the xylosyl side chains include a small proportion of xylosyl (1→2) xylose<sup>10</sup> disaccharide side chains in addition to those of single residues. Longer chains of xylose, up to seven residues in length, have been reported in soybean hull pectin.<sup>11</sup>

In most XGAs the xylose side chains prevent degradation of the homogalacturonan backbone by endopolygalacturonases (EPGs). However, we find that in watermelon, in at least some regions of the XGA, the xylose residues are spaced far enough apart that EPG can generate a range of oligosaccharides from it. We describe their structures here.

The mode of action of EPGs from fungi has been investigated several times. The size of the substrate binding site was deduced for an EPG from *Aspergillus niger* by looking at the rate of hydrolysis of different length oligomers of GalA.<sup>12</sup> The authors concluded that the binding site accommodated four residues, and hydrolysis took place between the third and fourth residues from the nonreducing end. Thibault<sup>13</sup> purified an EPG from *A. niger* and found that it randomly cleaves polygalacturonic acid to the monomer, dimer, and trimer of GalA, and that it could readily hydrolyze the tetramer of GalA to the trimer and monomer. One can conclude that a minimum of four residues need to bind to the enzyme and that it hydrolyzes between the third and fourth residues from the nonreducing end. Mort and Chen<sup>14</sup> compared the end products of hydrolysis of pectic acid by a commercial EPG from *A. niger* purchased from Megazyme International Ireland Ltd (as used in this study) and a cloned EPG from *Erwinia carotovora*. The enzyme from Megazyme gave the same products as observed by Thibault, but the bacterial enzyme produced predominantly the dimer, trimer, and tetramer. Thus it appears that the bacterial enzyme needs one more sugar unit bound to the active site of the enzyme and that it hydrolyzes between the third and fourth from the nonreducing end.

Bussink et al.<sup>15</sup> found that *A. niger* actually contains at least five genes for EPGs. It was suggested from high amino acid sequence homology and intron/exon structure that all of the genes evolved from one progenitor. Pel et al.<sup>16</sup> found eight genes for EPGs when the entire genome of the fungus was sequenced. The pattern of action of five EPGs from *A. niger* on polygalacturonic acid is very similar.<sup>17,18</sup> Some are progressive in their action, whereas others cleave randomly. One can easily imagine that methyl esterification, acetylation, xylosylation, or introduction of a sugar other than GalA in the galacturonan chain would have a dramatic effect on the positions at which the enzyme can hydrolyze. For example, Zhan et al.<sup>19</sup> found that the presence of altru-

ronic acid in the chain was not tolerated in any of the four essential sugar-binding sites of the Megazyme enzyme. Knowing the influence of xylose substituents on the susceptibility of xylogalacturonans to EPG will help understand XGA structure.

Several fungi produce an endoxylogalacturonan hydrolase that specifically requires xylose residues for its action.<sup>20,21</sup> The products of the hydrolysis are mostly very short oligomers.<sup>22</sup> The combination of EPG and xylogalacturonan hydrolase will be extremely useful for determining the structures of XGAs and their connections to homogalacturonans and/or rhamnogalacturonans.

## 2. Experimental

### 2.1. Preparation of xylogalacturonan oligomers

The pink flesh of de-seeded watermelons was homogenized in HEPES buffer at pH 7, and then enzymes were inactivated by suspension in Tris-buffered phenol or phenol–acetic acid–water.<sup>23</sup> The residue was washed with 80% ethanol, acetone, 1:1 chloroform–methanol, and finally acetone and then dried in an oven at 34 °C.

Xylogalacturonan oligomers were prepared from watermelon cell walls using slight modifications of the methods described previously.<sup>5</sup> Briefly, dry walls were suspended in 0.1 M NaOH at room temperature and the pH was maintained at 13 (as judged by pH paper) for 15 min and then incubated at 4 °C overnight. The soluble portion was collected after centrifugation, followed by neutralization with acetic acid, and dialysis against deionized water. After freeze-drying, the extract was digested with 0.05 units of endopolygalacturonase CAZY family 28 from *A. niger* (Megazyme catalog No. E\_PGALS) per mg extract for several days at 37 °C. According to the manufacturer the enzyme gave a single major band at MW = 24,000 and was very low in extraneous activities against other cell-wall polysaccharides. (Unfortunately this molecular weight does not match any of those reported for *A. niger* endopolygalacturonases.) In later experiments an EPG cloned from *Aspergillus nidulans* open reading frame AN8761.2<sup>20</sup> was used, and produced the same oligosaccharides. Both enzymes seem to be most like the PG II of *A. niger*. After heating to destroy the enzyme, the solution was passed through an ultrafiltration membrane with a 10-kD cutoff. What passed through the membrane was freeze-dried and passed through a Toyo-Pearl HW-40 gel-permeation column (22 × 500 mm in 50 mM NH<sub>4</sub>OAc buffer at a flow rate of 2 mL/min). The material eluting just after the void volume, but before the trimer of galacturonic acid, which was identified by capillary electrophoresis, was pooled. (See Fig. 4 in Ref. 5). It was fractionated on a 9 × 250-mm Dionex

PA1 column using a flow rate of 2 mL/min and a gradient from 30 mM to 350 mM  $\text{NH}_4\text{OAc}$  over 10 min, followed by an increase to 650 mM over the next 35 min, with a subsequent increase to 1 M over the next 15 min. A small fraction of the eluate (about 0.05) was split, using a needle valve splitter from Upchurch, to a permanganate-bleaching detector<sup>24</sup> for locating which fractions contained sugars. In the later experiments, the eluate was split using an analytical adjustable flow splitter from Analytical Scientific Instruments and analyzed using a Sedex 55 evaporative light-scattering detector. Peak fractions were pooled and freeze-dried three or four times to remove the  $\text{NH}_4\text{OAc}$ .

## 2.2. Instrumental methods

MALDI TOF mass spectrometry was performed on a Perkin–Elmer Voyager DE Pro instrument in the negative-ion reflector mode using 10% trihydroxyacetophenone in methanol as matrix. NMR spectra were collected on a Varian Unity Inova 600 MHz instrument using standard pulse sequences supplied with the instrument. 2D spectral data were processed using NMRPipe<sup>25</sup> and analyzed with NMRView.<sup>26</sup> Monosaccharide compositions of various fractions were determined by GLC of their trimethylsilyl methyl glycosides as described previously.<sup>27</sup> Electrospray-ionization tandem mass spectrometry (ESIMS/MS) was performed as described previously<sup>28</sup> on a Finnigan MAT TSQ 700 triple quadrupole mass spectrometer equipped with a Finnigan electrospray ion source (Finnigan MAT Corp., San Jose, CA). The reduced and permethylated samples were dissolved in acetonitrile saturated with NaCl and injected (concentrations approximately 10 pmol/ $\mu\text{L}$ ) at a flow rate of 1  $\mu\text{L}/\text{min}$  into the electrospray chamber. In the positive-ion mode, a voltage of +5.5 kV was applied to the electrospray needle. For collision-induced dissociation (CID) experiments, parent ions were selectively transmitted by the first mass analyzer and directed into the collision cell (Ar was used as collision gas) with a kinetic energy set around –60 eV. Native oligosaccharides were dissolved in MeOH containing 0.5%  $\text{NH}_3$  and subjected to negative-ion mode ESIMS. For the detection of negative-ions, all polarities were reversed, that is, –4.5 kV was applied to the needle and the collision energy was set at approximately +40 eV for MS/MS experiments.

## 3. Results and discussion

Watermelon cell walls were simultaneously saponified and extracted with 0.1 M NaOH to give a solubilized pectin fraction. This fraction had a molar ratio of around 7 GalA:1 Xyl:0.35 Rha, indicating that it contained a combination of rhamnogalacturonan (RG)

and homogalacturonan/xylogalacturonan. The extract was digested to completion with a commercial, purified endopolygalacturonase with known activity against polygalacturonic acid and partially esterified homogalacturonans. Progress of the hydrolysis was monitored by changes in the oligosaccharide product distribution seen by CZE of aliquots labeled with ANTS.<sup>14</sup> The products from the digestion contained high-molecular-weight RG and XGA, XGA fragments, and galacturonic acid oligomers.<sup>5</sup> After trying several different sequences of steps to enrich for relatively small xylogalacturonan oligomers, we settled on the scheme described in Section 2.1. The most efficient way we found to select for the XGA fragments was to first pass the EPG digest through a 10-kD cutoff ultrafiltration membrane to remove the RG and high-molecular-weight XGA, then to remove the very abundant  $\text{GalA}_{(1-3)}$  oligomers by the passage of the ultrafiltrate through an HW-40 gel-permeation column. Fortunately, the  $\text{GalA}_3$  oligomer eluted just after the bulk of the XGA oligomers, which eluted just after the void volume.

The XGA oligomers were fractionated on a semipreparative PA1 cation-exchange column; Figure 1 shows the profile of a material eluting from the PA1 column. Since the eluate was monitored by measuring the bleaching of a permanganate solution by the oxidation of the sugars, the relative peak area reflects the relative mass of sugar in each peak. The material eluting between 35 and 37 min (peak 7, the biggest peak) was collected and subjected to extensive NMR and mass spectral analysis. Compositional analysis showed it to contain almost exclusively GalA and Xyl.

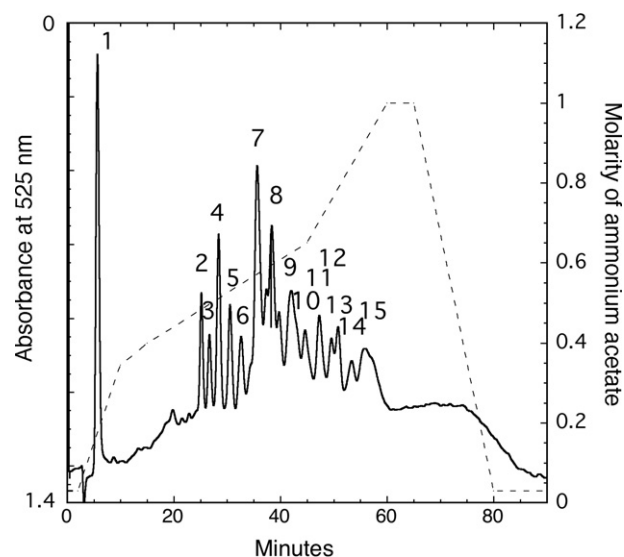


**Figure 1.** Fractionation of the xylose-rich oligosaccharides from watermelon pectin on a PA1 anion-exchange column. Sugars were detected by a decrease in absorbance at 525 nm caused by bleaching of permanganate as it oxidized the sugars.

Negative-ion mode electrospray-ionization mass spectrometry of the oligosaccharide in peak 7 of Figure 1 showed a peak at  $m/z$  1337.8, which corresponds well to  $[\text{HexA}_6\text{Pent}_2-\text{H}]$ . Three intense signals at 668.5, 679.4, and 690.6 are consistent with a doubly charged oligomer  $[-2\text{H}]$ , plus one, and plus two sodium ions, respectively, and another two signals at 445.4 and 452.8 are consistent with a triply charged oligomer  $[-3\text{H}]$  and plus one sodium ion. The MS/MS spectrum of the doubly charged oligosaccharide and a deduced fragmentation scheme are shown in Figure 2. The composition of the oligosaccharide can be deduced from the parent mass, whereas the monosaccharide sequence can be deduced from the fragment ions as is explained in the inserted scheme. The MS/MS spectrum of the reduced and permethylated sodiated oligosaccharide and a proposed fragmentation scheme are shown in Figure 3. Two complete and complementary fragment ion series from the reduced and nonreducing end of the molecule allow the deduction of the monosaccharide sequence. The attachment points of the two pentose residues to the hexuronic acid main chain can be directly determined from the corresponding mass jump of the respective fragment ions as is explained in the inserted scheme. The observed secondary elimination of these pentose residues does not lead to ambiguities, since the corresponding fragments carry one methyl group less than

fragments generated from a hypothetical linear chain. Both MS/MS spectra indicate that the oligosaccharide consists of a linear chain of six hexuronic acids with a pentose attached to the first and third uronic acids in the chain (counting from the nonreducing terminus).

In the 1D  $^1\text{H}$  NMR spectrum of the oligosaccharide in peak 7 of Figure 1, there were three clear signals corresponding to the anomeric protons of  $\beta$ -pyranoses (4.53, 4.62, and 4.66 ppm), a cluster of signals where one would expect those of  $\alpha$ -linked GalA residues (5.1 ppm) and one for a reducing  $\alpha$ -GalA (5.32 ppm). From the COSY, TOCSY, and HMQC spectra, we could identify the large majority of the H and C chemical shifts of the oligosaccharide (see Fig. 4 and Table 1). There were clearly two sets of signals for the xylose residues and two GalA residues in which the C-3 resonances were downfield of those normally found in GalA oligomers. The proposed structure of the oligosaccharide is shown in Figure 5. From the HMBC spectrum (Fig. 6) one can deduce that the xylose residue with H-1 at 4.66 ppm was attached to C-3 (A1, B3 at 4.66, 79.02) of the nonreducing end GalA residue (with its C-4 resonance, B4, at 70.91 ppm). The other xylose residue is linked to C-3 of GalA residue D (H1, D3 at 4.53, 78.13). The C-4 resonance of residue D is at 76.74, reflecting the downfield shift induced by its glycosidic linkage to a GalA residue and a slight upfield shift

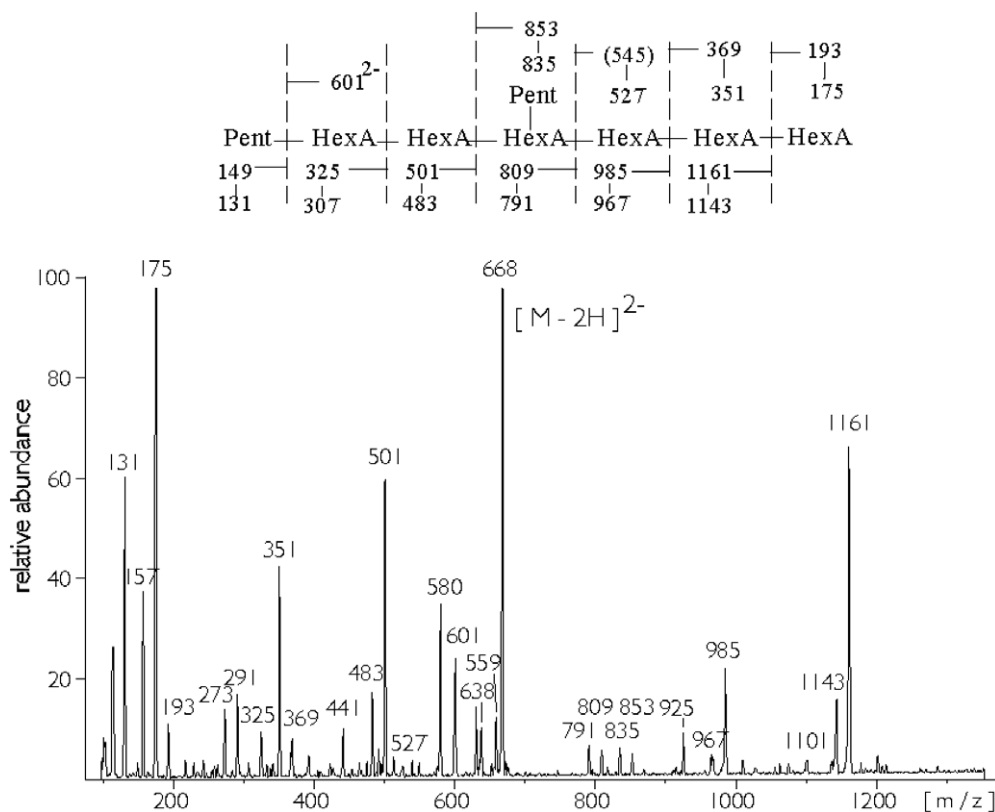
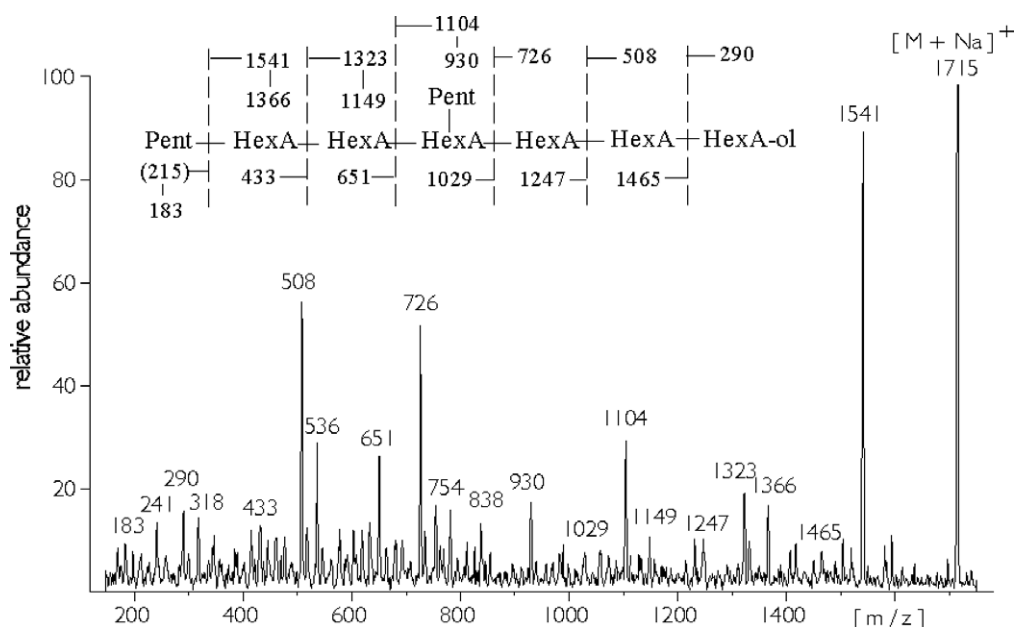
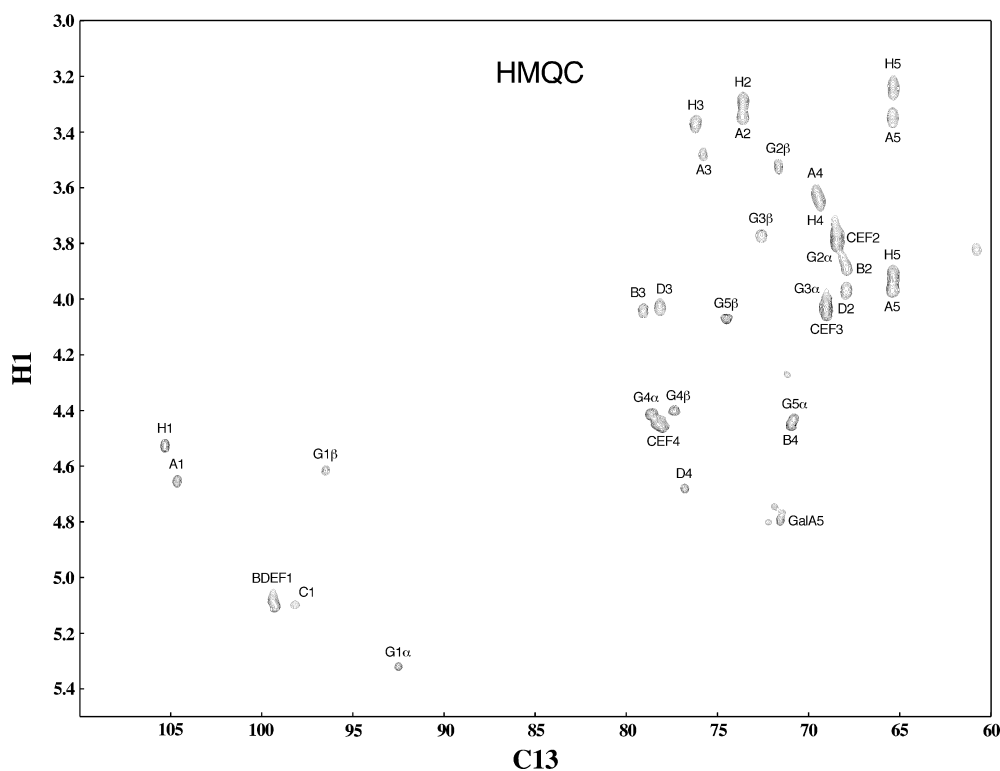


Figure 2. Negative daughter-ion spectrum of the doubly charged molecular ion ( $m/z$  668.5) of an octasaccharide obtained from ion-exchange chromatography (fraction 7) and the deduced fragmentation pattern.



**Figure 3.** Positive daughter-ion spectrum of the singly charged sodium adduct of the reduced ( $\text{NaBD}_4$ ) and permethylated oligosaccharide from fraction 7 and the deduced fragmentation scheme.



**Figure 4.** HMQC spectrum of fraction 7.

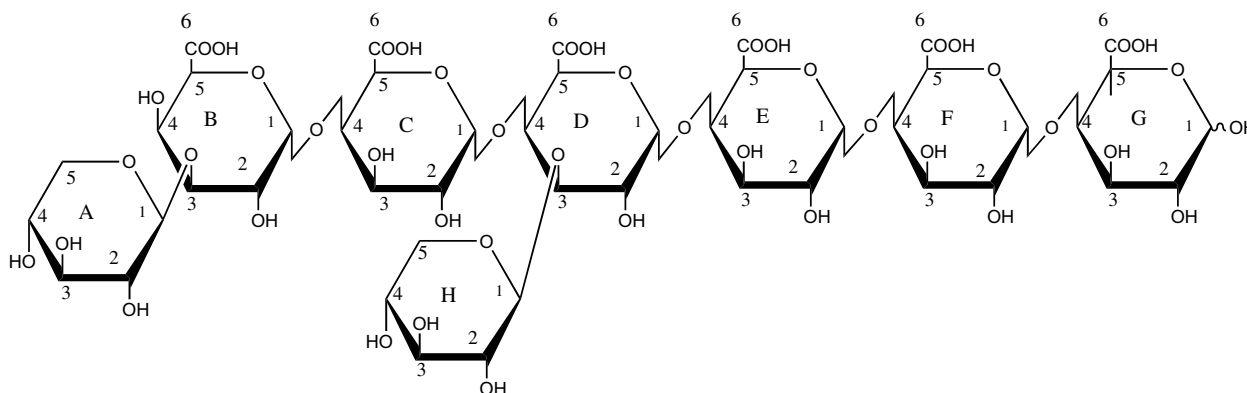
because of the adjacent C-3 glycosidic linkage from xylose. The chemical shifts of the other GalA residues are very close to those reported for linear GalA oligomers<sup>29</sup> except that C-1 and C-4 of residue C are a little more than 1 ppm upfield. The NMR results confirm

the MS/MS identification of the oligosaccharide being a linear chain of GalA residues with a single xylose attached to the nonreducing terminal GalA and another attached to the third GalA in the chain. They also confirm that the GalA residues are linked via  $\alpha$ -(1→4)



**Table 1.**  $^1\text{H}$  and  $^{13}\text{C}$  NMR chemical shifts for the oligosaccharide eluting in peak 7 from the PA1 column

Residue		1	2	3	4	5	6
A	$\beta\text{-D-Xylp-(1}\rightarrow$	4.66	3.34	3.48	3.62	3.35, 3.97	
		104.62	73.58	75.75	69.53	65.37	
B	$\rightarrow 3)\text{-}\alpha\text{-D-GalAp-(1}\rightarrow$	5.08	3.88	4.04	4.47	4.80	175.97
		99.37	67.93	79.02	70.91	72.25	
C	$\rightarrow 4)\text{-}\alpha\text{-D-GalAp-(1}\rightarrow$	5.10	3.74	4.03	4.44	4.773	175.97
		98.15	68.53	68.99	78.35	77.228	
D	$\rightarrow 3,4)\text{-}\alpha\text{-D-GalAp-(1}\rightarrow$	5.08	3.97	4.03	4.68	4.74	175.72
		99.37	67.93	78.13	76.74	65.37	
E	$\rightarrow 4)\text{-}\alpha\text{-D-GalAp-(1}\rightarrow$	5.11	3.79	4.03	4.46	4.80	175.97
		99.29	68.46	68.99	78.05	71.52	
F	$\rightarrow 4)\text{-}\alpha\text{-D-GalAp-(1}\rightarrow$	5.11	3.79	4.03	4.46	4.80	175.97
		99.29	68.46	68.99	78.05	71.52	
G- $\alpha$	$\rightarrow 4)\text{-}\alpha\text{-GalAp}$	5.32	3.84	3.97	4.41	4.44	175.538
		92.50	68.30	68.99	78.62	70.79	
G- $\beta$	$\rightarrow 4)\text{-}\beta\text{-GalAp}$	4.62	3.53	3.77	4.40	4.07	174.76
		96.48	71.62	72.55	77.33	74.44	
H	$\beta\text{-D-Xylp-(1}\rightarrow$	4.53	3.29	3.37	3.65	3.24, 3.92	
		105.29	73.58	76.15	69.33	65.34	

**Figure 5.** Structure of the oligosaccharide in fraction 7.

linkages and that the xylose residues are linked via  $\beta$ -linkages to O-3 of GalA residues.

In one experiment, 1-min fractions of the eluate from the PA1 column were collected individually and most were analyzed by MALDI TOF mass spectrometry. Table 2 gives the masses of the major peaks observed and the tentative identifications of each. For fractions corresponding to peaks 4 and 6 of Figure 1, the structures were confirmed by NMR spectroscopy. The  $^1\text{H}$  spectrum of the pentasaccharide in peak 4 (fractions 25–27) showed the signals one would expect for an  $\alpha$ -(1 $\rightarrow$ 4)-GalA oligomer with additional signals almost identical to those assigned to the  $\beta$  xylose on the non-reducing end of the xylogalacturonan oligomer discussed above (H-1, 4.64; H-2, 3.34; H-3, 3.47; H-4, 3.62; H-5, 3.34). A signal at 4.27 ppm, characteristic of an unsubstituted nonreducing end GalA, was not present, just as was the case in the GalA<sub>6</sub>Xyl<sub>2</sub> oligomer. Thus, the oligomer in peak 4 must be XOOO, where ‘O’ denotes a GalA residue and ‘X’ denotes a xylosylated GalA resi-

due. The  $^1\text{H}$  spectrum of the hexasaccharide in fraction 30 (peak 6 of Fig. 1) had a signal at 4.27 ppm and signals identical to those of the xylose on the internal GalA in the GalA<sub>6</sub>Xyl<sub>2</sub> oligomer, that is, H-1, 4.53; H-2, 3.29; H-3, 3.37; H-4, 3.63, and H-5 not resolved. This oligomer must be OXOOO. Several trends were clear in the behavior of the oligomers: The more GalA residues in the oligomer, the higher ionic strength needed to elute them, and for an oligomer containing a particular number of GalA residues, more xylose residues caused earlier elution. For example, GalA<sub>5</sub>Xyl<sub>2</sub> eluted before GalA<sub>6</sub>Xyl<sub>2</sub>, and GalA<sub>5</sub>Xyl<sub>2</sub> eluted before GalA<sub>5</sub>Xyl<sub>1</sub>.

One major oligomer (peak 3 of Fig. 1, fraction 24 in Table 2) and several minor ones had masses in the negative-ion MALDI TOF spectrum that were even, for example,  $m/z$  1000.3 for peak 3–H. Since all oligosaccharides, unless they contain amino sugars, have odd masses, this indicated the presence of nitrogen. The  $^1\text{H}$  NMR spectrum of the oligomer in peak 3 showed no evidence of common amino sugars, but did display



**Table 2.** Mass spectral characterization of PA1 column eluate

Fraction no. <sup>a</sup>	Mass <sup>b</sup>	Composition	Potential structure <sup>c</sup>
22	545.12, 567.1	GalA <sub>3</sub> -H	OOO
23	545.16	GalA <sub>3</sub> -H	OOO
(Peak 3) 24	1000.5, 1022.48	GalA <sub>5</sub> _Tris-amide-H	OTOOO
(Peak 4) 25	853.51	GalA <sub>4</sub> Xyl-H	XOOO
(Peak 4) 26	853.27	GalA <sub>4</sub> Xyl-H	XOOO
(Peak 4) 27	853.31	GalA <sub>4</sub> Xyl-H	XOOO
	1161.45, 1183.42	GalA <sub>5</sub> Xyl <sub>2</sub> -H	XXOOO
	1308.5, 1330.5	GalA <sub>5</sub> Xyl_Tris-amide-H	XTOOO
28	1161.59, 1183.62	GalA <sub>5</sub> Xyl <sub>2</sub> -H	XXOOO
29	1161.18	GalA <sub>5</sub> Xyl <sub>2</sub> -H	XXOOO
	1176.19, 1198.18	GalA <sub>6</sub> _Tris-amide-H	OXTOOO
	1469.17, 1491.17	GalA <sub>6</sub> Xyl <sub>3</sub> -H	XXXOOO
	1616.17	GalA <sub>7</sub> Xyl <sub>2</sub> _Tris-amide-H	XOXTOOO ?
(Peak 6) 30	1029.3, 1051.3, 1067.3	GalA <sub>5</sub> Xyl-H	OXOOO
	1176.37, 1198.3	GalA <sub>6</sub> _Tris-amide-H	OOTOOO
	1469.4, 1491.37	GalA <sub>6</sub> Xyl <sub>3</sub> -H	XXXOOO
31	1029.4, 1051.3	GalA <sub>5</sub> Xyl-H	OXOOO
	1337.4	GalA <sub>6</sub> Xyl <sub>2</sub> -H	XOXOOO
	1484.5, 1506.5	GalA <sub>6</sub> Xyl_Tris-amide-H	XOTOOO ?
	1777.5	GalA <sub>7</sub> Xyl <sub>4</sub> -H	XXXXOOO
	1924.6	GalA <sub>9</sub> Xyl <sub>2</sub> _Tris-amide-H	XOXOOTOOO ?
(Peak 7) 32	1337.5	GalA <sub>6</sub> Xyl <sub>2</sub> -H	XOXOOO
(Peak 7) 33	1337.67, 1359.5	GalA <sub>6</sub> Xyl <sub>2</sub> -H	XOXOOO
(Peak 7) 34	1337.28, 1359.3	GalA <sub>6</sub> Xyl <sub>2</sub> -H	XOXOOO
	1645.35	GalA <sub>7</sub> Xyl <sub>3</sub> -H	XOXXXXO ?
35	1205.24, 1227.21	GalA <sub>6</sub> Xyl-H	OOXOOO
	1645.35, 1667.32	GalA <sub>7</sub> Xyl <sub>3</sub> -H	XOXXXXO ?
36	1205.37, 1227.28, 1243.25	GalA <sub>6</sub> Xyl-H	OOXOOO
	1953.26	GalA <sub>8</sub> Xyl <sub>4</sub> -H	XOXOXOOO ?
37	1513.5, 1535.49	GalA <sub>7</sub> Xyl <sub>2</sub> -H	OXOXOOO ?
38	1513.6, 1535.59	GalA <sub>7</sub> Xyl <sub>2</sub> -H	OXOXOOO ?
	1821.69, 1843.65	GalA <sub>8</sub> Xyl <sub>3</sub> -H	XOXOXOOO ?
39	1513.66	GalA <sub>7</sub> Xyl <sub>2</sub> -H	OOXXXXO ?
	1645.73	GalA <sub>7</sub> Xyl <sub>3</sub> -H	XOXXXXO ?
	1821.75, 1843.73	GalA <sub>8</sub> Xyl <sub>3</sub> -H	XOXOXOOO ?
	2129.86	GalA <sub>9</sub> Xyl <sub>4</sub> -H	XOXOXOOO ?
40	1821.39	GalA <sub>8</sub> Xyl <sub>3</sub> -H	
	2129.46	GalA <sub>9</sub> Xyl <sub>4</sub> -H	
41	897.5, 919.49	GalA <sub>5</sub> -H	
	1205.65, 1227.59	GalA <sub>6</sub> Xyl <sub>1</sub> -H	
	1513.77, 1535.59	GalA <sub>7</sub> Xyl <sub>2</sub> -H	
	1689.8	GalA <sub>8</sub> Xyl <sub>2</sub> -H	
	1821.84	GalA <sub>8</sub> Xyl <sub>3</sub> -H	
	2129.9	GalA <sub>9</sub> Xyl <sub>4</sub> -H	
42	1513.38	GalA <sub>7</sub> Xyl <sub>2</sub> -H	
	1689.39, 1711.36, 1733.36	GalA <sub>8</sub> Xyl <sub>2</sub> -H	
43	1689.53, 1711.5	GalA <sub>8</sub> Xyl <sub>2</sub> -H	
	1997.6	GalA <sub>9</sub> Xyl <sub>3</sub> -H	
44	1821.63	GalA <sub>8</sub> Xyl <sub>3</sub> -H	
	1997.5	GalA <sub>9</sub> Xyl <sub>3</sub> -H	
	2129.73	GalA <sub>9</sub> Xyl <sub>4</sub> -H	
	2305.8, 2327.65	GalA <sub>10</sub> Xyl <sub>4</sub> -H	
	2613.65	GalA <sub>11</sub> Xyl <sub>5</sub> -H	
45	2129.46	GalA <sub>9</sub> Xyl <sub>4</sub> -H	
	2305.52, 2327.42	GalA <sub>10</sub> Xyl <sub>4</sub> -H	
	2613.42, 2635.3	GalA <sub>11</sub> Xyl <sub>5</sub> -H	
	2921.64, 2943.13	GalA <sub>12</sub> Xyl <sub>6</sub> -H	

<sup>a</sup> Fraction numbers are 1-min fractions from the PA1 column; peak numbers refer to Figure 1. The fraction numbers and elution times in Figure 1 are offset by 3 min because of the time it takes for the samples to pass through the reaction coil of the permanganate detection system.

<sup>b</sup> The second number in this column is  $m/z$  [M-H+Na] and the third (if present) is  $m/z$  [M-H+K].

<sup>c</sup> 'O' denotes a GalA residue; 'X' a xylosylated GalA residue; 'T' a GalA residue with Tris in amide linkage; '?' other structures are also consistent with the data.



**Table 3.**  $^1\text{H}$  and  $^{13}\text{C}$  NMR chemical shifts for the oligosaccharide eluting in peak 3 from the PA1 column

Residue	1	2	3	4	5
→4)- $\alpha$ -D-GalAp-(1→	5.073	3.794	3.932	4.277	4.756
	99.228	68.595	69.859	70.893	72.541
→4,6)- $\alpha$ -D-GalAp-(1→	5.177	3.817	4.056	4.515	4.851
	99.625	68.251	68.595	75.717	71.330
→4,6)- $\alpha$ -D-GalAp-(1→	5.161	3.817	4.056	4.515	4.851
	99.743	68.251	68.595	78.359	71.330
→4)- $\alpha$ -D-GalAp-(1→	5.072	3.791	4.501	4.436	4.800
	99.034	68.251	72.031	79.933	71.472
→4)- $\alpha$ -D-GalAp-(1→	5.098	3.755	4.012	4.427	4.748
	99.269	72.501	69.055	78.703	71.543
→4)- $\alpha$ -GalAp	5.320	3.852	4.011	4.439	4.427
	92.845	68.366	69.055	78.933	70.718
→4)- $\beta$ -GalAp	4.622	3.517	3.764	4.400	4.056
	96.474	71.697	72.501	78.014	74.339

Megazyme can recognize and cleave homogalacturonans as short as four GalA residues so long as they are not methyl esterified. The bond between the third and fourth residues is the one which is hydrolyzed. We were surprised to find that the most abundant XGA oligomers this EPG produces from the XGA of watermelon have a Xyl residue at their nonreducing ends. It appears that the position in the active site of the enzyme that binds the last of the four residues can accommodate a xylose residue on O-3 of the GalA residue. On the other hand, the other three positions appear not to be able to accommodate xylose side branches, since there are always three nonxylosylated GalA residues at the reducing end of the oligomers. The presence of oligomers starting with a nonsubstituted GalA indicates that there must have been some regions in the original XGA polymer with at least four adjacent nonxylosylated GalA residues. In the case of Tris-amidated pectin, the Tris cannot be accommodated in the active site of the enzyme, so the smallest oligomer containing Tris must start with an unsubstituted GalA and end in three unsubstituted GalA residues.

### Acknowledgments

This work was supported by DOE Grant DE-FG02-96ER20215 and has been approved for publication by the Director of the Oklahoma Agricultural Experiment Station. We thank Margaret Pierce for comments on the manuscript and help in putting it together.

### References

- Bouveng, H. O. *Acta Chem. Scand.* **1965**, *19*, 953–963.
- Stephen, A. M. In *The Polysaccharides*; Aspinall, G. O., Ed.; Academic Press: New York, 1983; Vol. 2, pp 97–193.
- Schols, H. A.; Bakx, E. J.; Schipper, D.; Voragen, A. G. J. *Carbohydr. Res.* **1995**, *279*, 265–279.
- Schols, H. A.; Voragen, A. G. J. *Carbohydr. Res.* **1994**, *256*, 83–95.
- Yu, L.; Mort, A. J. *Prog. Biotechnol.* **1996**, *14*, 79–88.
- Albersheim, P.; Darvill, A. G.; O'Neill, M. A.; Schols, H. A.; Voragen, A. G. J. *Prog. Biotechnol.* **1996**, *14*, 47–55.
- Kikuchi, A.; Edashige, Y.; Ishii, T.; Satoh, S. *Planta* **1996**, *200*, 369–372.
- Zandleven, J.; Sorensen, S. O.; Harholt, J.; Beldman, G.; Schols, H. A.; Scheller, H. V.; Voragen, A. J. *Phytochemistry* **2007**, *68*, 1219–1226.
- Mort, A. J. In *Pectins and their Manipulation*; Seymour, G. B., Knox, J. P., Eds.; Blackwell: Sheffield, 2002; pp 30–51.
- Le Goff, A.; Renard, C. M. G. C.; Bonnin, E.; Thibault, J. F. *Carbohydr. Polym.* **2001**, *45*, 325–334.
- Nakamura, A.; Furuta, H.; Maeda, H.; Takao, T.; Nagamatsu, Y. *Biosci., Biotechnol., Biochem.* **2002**, *66*, 1155–1158.
- Rexová-Benková, L'. *Eur. J. Biochem.* **1973**, *39*, 109–115.
- Thibault, J. F. *Carbohydr. Polym.* **1983**, *3*, 259–272.
- Mort, A. J.; Chen, E. M. W. *Electrophoresis* **1996**, *17*, 379–383.
- Bussink, H. J. D.; Burton, F. P.; Fraaye, B. A.; de Graaff, L. H.; Visser, J. *Eur. J. Biochem.* **1992**, *208*, 83–90.
- Pel, H. J.; de Winde, J. H.; Archer, D. B.; Dyer, P. S.; Hofmann, G.; Schaap, P. J.; Turner, G.; de Vries, R. P.; Albang, R.; Albermann, K.; Andersen, M. R.; Bendtsen, J. D.; Benen, J. A. E.; van den Berg, M.; Breestraat, S.; Caddick, M. X.; Contreras, R.; Cornell, M.; Coutinho, P. M.; Danchin, E. G. J.; Debets, A. J. M.; Dekker, P.; van Dijk, P. W. M.; van Dijk, A.; Dijkhuizen, L.; Driessen, A. J. M.; d'Enfert, C.; Geysens, S.; Goosen, C.; Groot, G. S. P.; de Groot, P. W. J.; Guillemette, T.; Henrissat, B.; Herweijer, M.; van den Hombergh, J. P. T. W.; van den Hondel, C. A. M. J. J.; van der Heijden, R. T. J. M.; van der Kaaij, R. M.; Klis, F. M.; Kools, H. J.; Kubicek, C. P.; van Kuyk, P. A.; Lauber, J.; Lu, X.; van der Maarel, M. J. E. C.; Meulenber, R.; Menke, H.; Mortimer, M. A.; Nielsen, J.; Oliver, S. G.; Olsthoorn, M.; Pal, K.; van Peij, N. N. M. E.; Ram, A. F. J.; Rinas, U.; Roubos, J. A.; Sagt, C. M. J.; Schmoll, M.; Sun, J.; Ussery, D.; Varga, J.; Vervecken, W.; van de Vondervoort, P. J. J.; Wedler, H.; Woesten, H. A. B.; Zeng, A.-P.; van Ooyen, A. J. J.; Visser, J.; Stam, H. *Nat. Biotechnol.* **2007**, *25*, 221–231.
- Benen, J. A. E.; Kester, H. C. M.; Visser, J. *Eur. J. Biochem.* **1999**, *259*, 577–585.

18. Parenicova, L.; Benen, J. A. E.; Kester, H. C. M.; Visser, J. *Biochem. J.* **2000**, *345*, 637–644.
19. Zhan, D.; Qiu, F.; Mort, A. J. *Carbohydr. Res.* **2001**, *330*, 357–363.
20. Bauer, S.; Vasu, P.; Persson, S.; Mort, A. J.; Somerville, C. R. *Proc. Natl. Acad. Sci. U.S.A.* **2006**, *103*, 11417–11422.
21. Van der Vlugt-Bergmans, C. J. B.; Meeuwsen, P. J. A.; Voragen, A. G. J.; Van Ooyen, A. J. J. *Appl. Environ. Microbiol.* **2000**, *66*, 36–41.
22. Zandleven, J.; Beldman, G.; Bosveld, M.; Benen, J.; Voragen, A. *Biochem. J.* **2005**, *387*, 719–725.
23. Huber, D. J. *Phytochemistry* **1991**, *30*, 2523–2527.
24. Thomas, J.; Mort, A. J. *Anal. Biochem.* **1994**, *223*, 99–104.
25. Delaglio, F.; Grzesiek, S.; Vuister, G. W.; Zhu, G.; Pfeifer, J.; Bax, A. *J. Biomol. NMR* **1995**, *5*, 277–293.
26. Johnson, B. A.; Blevins, R. A. *J. Biomol. NMR* **1994**, *4*, 603–614.
27. Zhang, Z.; Pierce, M. L.; Mort, A. J. *Phytochemistry* **2007**, *68*, 1094–1103.
28. Nimtz, M.; Mort, A.; Domke, T.; Wray, V.; Zhang, Y.; Qiu, F.; Coplin, D.; Geider, K. *Carbohydr. Res.* **1996**, *287*, 59–76.
29. Lo, V.-M.; Hahn, M. G.; van Halbeck, H. *Carbohydr. Res.* **1994**, *255*, 271–284.
30. Perrone, P.; Hewage, C. M.; Sadler, I. H.; Fry, S. C. *Phytochemistry* **1998**, *49*, 1879–1890.